Research Square

Preprints are preliminary reports that have not undergone peer review.
They should not be considered conclusive, used to inform clinical practice,
or referenced by the media as validated information.

Desilting 4.0: A Sky–Land–Water–AI Digital-Twin Framework for Low-Emission Multi-Contaminant Co-Solidification and Machine-Learning Foresight in El Niño-Ready Andean Rivers and Lagoons

PAUL RICARDO PRUDENCIO GALVEZ

pprudencio@autonoma.edu.pe

Universidad Autónoma del Perú

Method Article

Keywords: low-emission binders, solidification/stabilization, multi-contaminant co-solidification, machine learning, sediment strength and leachability forecasting, Sky–Land–Water–AI monitoring, river and lagoon descolmatation, El Niño, Peruvian Andes

Posted Date: August 28th, 2026

DOI: https://doi.org/10.21203/rs.3.rs-10375134/v1

License: This work is licensed under a Creative Commons Attribution 4.0 International License.
Read Full License

Additional Declarations: No competing interests reported.

Abstract

Descolmatation (desilting) of Andean rivers and lagoons in Peru routinely encounters sediment that is jointly loaded with heavy metals and organic pollutants, a co-contamination pattern that conventional single-binder, single-contaminant remediation designs do not address. This Method Article synthesizes documented, DOI-verified evidence on (i) low-emission composite binders (ground granulated blast-furnace slag, fly ash, carbide slag and organic amendments) and their micro-scale immobilization mechanisms, (ii) multi-model machine-learning (ML) ensembles for forecasting unconfined compressive strength (UCS) and leachability trends in stabilized soils and sediments, (iii) an integrated Sky–Land–Water–AI monitoring architecture adapted from space–air–ground remote-sensing networks documented for Chinese river basins, and (iv) co-solidification strategies for simultaneous heavy-metal and organic-contaminant immobilization documented in Chinese case studies. Building on this evidence base, the article proposes an integrated engineering framework formalized through four governing relations: an exponential strength–binder-ratio law, a solid–liquid partition/immobilization coefficient for co-contaminants, a weighted multi-model ML ensemble equation for trend forecasting, and a carbon-footprint reduction metric. A comparative matrix contrasts documented Asian (predominantly Chinese) full-scale and pilot practice against a proposed low-cost, solar-powered, modular configuration adapted to the topography, intermittent grid access and El Niño-driven hydrological variability of Andean rivers and lagoons in Peru, illustrated with documented water-quality evidence from the Rimac and Ichu river basins. As of mid-2026, Peru's National Committee for the Study of the El Niño Phenomenon (ENFEN) and the World Meteorological Organization have flagged a high probability of an El Niño event with intensified rainfall and riverbed sedimentation, which motivates the urgency of scalable descolmatation technology. The framework is presented as a design-and-synthesis proposal rather than a validated field trial; pilot-scale validation with Peruvian field data is identified as the necessary next step. No human or animal subjects were involved, and no primary biological or clinical data were collected.

1. Introduction

Rivers, lakes and lagoons in mining-influenced and rapidly urbanizing watersheds accumulate sediment that combines heavy metals with organic pollutants, and this sediment must be periodically removed through descolmatation works before it can be safely reused or disposed of (Yang et al. 2022; Gao et al. 2023). Portland-cement-based stabilization/solidification (S/S) remains the most widely deployed remediation technology for such sediment, but conventional ordinary Portland cement (OPC) treatment carries a high carbon footprint and can itself introduce alkalinity and leaching risks, motivating a shift toward low-emission composite binders such as ground granulated blast-furnace slag (GGBS), fly ash and carbide slag (Wang et al. 2018).

In parallel, predicting the unconfined compressive strength (UCS) and long-term leachability of stabilized sediment has moved from single empirical curing curves toward multi-model machine-learning ensembles that combine several algorithms (random forest, gradient boosting, extreme gradient

boosting, deep neural networks) to reduce predictive uncertainty and to forecast strength-development trends before full curing is complete (Abdullah et al. 2024; Zhang et al. 2026; Luo et al. 2025).

Monitoring the river or lagoon system that supplies the sediment has, in turn, moved toward integrated "space–air–ground" (here termed Sky–Land–Water–AI) remote-sensing and Internet-of-Things (IoT) architectures that combine satellite, drone and ground-based sensing with artificial-intelligence analysis, as documented for the Yellow River basin (Hou et al. 2024) and for smart-city water-quality IoT systems (Chen et al. 2023).

A further documented line of Asian practice addresses co-contamination directly: combined solidification/stabilization and chemical-oxidation treatments have been used in China to immobilize heavy metals and organic pollutants within the same treatment train (Ma et al. 2018), and humus-amended cement stabilization has been documented to reduce the exchangeable, bioavailable fraction of heavy metals in river sediment in Shanghai (Gao et al. 2023).

Gap and contribution. The low-emission binder literature, the ML strength/leachability forecasting literature, the Sky–Land–Water–AI monitoring literature and the co-solidification literature have developed largely as separate strands, with few frameworks that couple them into a single, jointly engineered descolmatation system — and fewer still that translate documented Asian full-scale and pilot experience into a configuration adapted to Andean field conditions. This is a significant limitation for Peru, where the Rimac and Ichu basins already exhibit heavy-metal pollution indices above critical contamination thresholds (Minga et al. 2023; Zárate-Cáceres et al. 2026), and where the Peruvian government and ENFEN have identified river and quebrada descolmatation as a priority preventive measure ahead of the El Niño 2026 rainy season. The contribution of this article is fourfold: (i) it compiles and compares documented, DOI-verified quantitative and procedural evidence on low-emission binders, ML-based trend forecasting, Sky–Land–Water–AI monitoring and multi-contaminant co-solidification into a single comparative matrix contrasting Asian practice against a Peru-adapted configuration; (ii) it formalizes the coupling between binder dosing, contaminant partitioning and ML forecasting through four governing formulas; (iii) it proposes a low-cost, solar-powered, modular deployment adapted to the topography, intermittent grid access and El Niño-driven hydrological variability of Andean rivers and lagoons in Peru; and (iv) it discusses how such a system could plausibly be adopted by water-utility and river-basin-management entities, and outlines the additional validation steps required before operational deployment.

2. Materials and Methods

This section describes the materials, computational tools and governing formulas used to build the proposed framework, together with the procedure used to compile and compare documented evidence from Asia and Peru. As this is a design-synthesis Method Article rather than a primary field or laboratory study, no new solidification, leaching or sediment-forecasting experiments were performed by the author;

all quantitative and procedural values reported in Section 3 are drawn directly from the cited, DOI-verified sources.

2.1 Materials and binders considered

Low-emission binder candidates: ground granulated blast-furnace slag (GGBS), Class-F fly ash and carbide slag, used individually or in composite blends to partially replace ordinary Portland cement (OPC) and reduce curing alkalinity while maintaining strength development (Wang et al. 2018). Organic soil amendments such as commercial humus have been documented to reduce the exchangeable fraction of heavy metals in river sediment when combined with cement-based solidification (Gao et al. 2023). Computational tools: Python-based machine-learning libraries (scikit-learn, XGBoost, TensorFlow) for the multi-model ensemble, following architectures documented for geopolymer- and cement-stabilized soils (Abdullah et al. 2024; Zhang et al. 2026); open hydrological and remote-sensing processing environments for basin-scale characterization. Instrumentation: in-situ hyperspectral and multispectral sensors for suspended-sediment concentration retrieval, together with turbidity, pH and dissolved-oxygen probes for local water-quality monitoring, consistent with the sensing approaches documented by Hou et al. (2024) and Chen et al. (2023).

2.2 Governing formulas

A. Empirical strength–binder-ratio law.

$$UCS = A \cdot \exp(-B \cdot (w/b))$$

where UCS is the unconfined compressive strength of the stabilized sediment (kPa), w/b is the water-to-binder ratio, and A and B are empirical fitting constants that depend on the binder blend and curing time; this exponential (Abrams-type) form is the functional shape most frequently fitted in the cement- and geopolymer-stabilized-soil literature synthesized here (Zhang et al. 2026; Abdullah et al. 2024).

B. Solid–liquid partition and immobilization efficiency for co-contaminants.

$$K_{d,i} = C_{s,i} / C_{l,i} \qquad \eta_i = [(C_{0,i} - C_{l,i}) / C_{0,i}] \times 100$$

where, for contaminant i (a given heavy metal or organic pollutant), $C_{s,i}$ and $C_{l,i}$ are its equilibrium solid-phase and leachate concentrations after solidification, $K_{d,i}$ is the resulting partition coefficient, $C_{0,i}$ is its initial (pre-treatment) concentration, and η_i is the percentage immobilization efficiency; higher $K_{d,i}$ and η_i indicate more effective co-contaminant immobilization within the solidified matrix, consistent with the combined solidification/chemical-oxidation results reported for co-contaminated Chinese soils (Ma et al. 2018).

C. Multi-model machine-learning ensemble for trend forecasting.

$\hat{y} = \Sigma(i=1..n)\ w_i \cdot f_i(X) \qquad w_i = (1/RMSE_i) / \Sigma(k=1..n)\ (1/RMSE_k)$

where $f_i(X)$ is the prediction of base model i (e.g., random forest, gradient boosting, extreme gradient boosting, or a recurrent/deep-learning model) for input feature vector X (curing time, binder content, water content, contaminant concentration, sediment grain-size), $RMSE_i$ is that model's root-mean-square error under cross-validation, and w_i is its inverse-RMSE weight; this ensemble form follows the weighting logic documented across several boosting- and deep-learning-based UCS-prediction studies synthesized here (Abdullah et al. 2024; Zhang et al. 2026; Luo et al. 2025).

D. Carbon-footprint reduction metric.

$CFred\ (\%) = [(CF_{OPC} - CF_{composite}) / CF_{OPC}] \times 100$

where CF_{OPC} is the carbon footprint per functional unit (e.g., per 100 kPa of achieved strength) of a pure-OPC-stabilized reference mix, and $CF_{composite}$ is the corresponding carbon footprint of the low-emission composite binder mix; this metric is the standard basis on which low-carbon binder substitution is evaluated in the sediment- and soil-stabilization literature (Wang et al. 2018).

2.3 Sky–Land–Water–AI monitoring architecture

The proposed monitoring architecture (Figure 1) couples four sensing layers — Sky (satellite remote sensing of suspended-sediment concentration), Air (drone-based hyperspectral and RGB survey), Land (ground-based hyperspectral or IoT stations recording turbidity, pH, dissolved oxygen and water level) and Water (in-situ sampling of sediment and co-contaminants) — with the multi-model ML ensemble described in Section 2.2, which forecasts UCS, leachability and turbidity trends and feeds a low-emission-binder dosing controller. This layered configuration follows the space–air–ground integrated remote-sensing network documented for suspended-sediment monitoring in the Yellow River basin (Hou et al. 2024) and the IoT-based, solar-powered water-level and water-quality control architecture documented for smart-city ponds (Chen et al. 2023).

2.4 Comparative procedure: Asian practice versus proposed adaptation for Peru

In documented Chinese full-scale and pilot deployments, low-emission composite binders are dosed in centralized batching plants with laboratory-supported quality control, and co-contaminated sediment (heavy metals plus organics) is treated through combined solidification/stabilization and chemical-oxidation trains supported by continuous grid power and paved site access (Wang et al. 2018; Ma et al. 2018; Gao et al. 2023). Yellow River basin monitoring similarly assumes a well-resourced network of satellite tasking, drone operations and permanently powered ground hyperspectral stations (Hou et al. 2024).

Andean rivers and lagoons in Peru present a different operating envelope: intermittent or absent grid power at high altitude, seasonal and El Niño-amplified flow variability, steep and often unpaved access, and heavy-metal loads originating from legacy and active mining activity that must be addressed jointly with organic micropollutants and with the accelerated sedimentation associated with El Niño rainfall (Minga et al. 2023; Zárate-Cáceres et al. 2026).

The proposed adaptation (Figure 2) therefore replaces centralized batching plants with a mobile mixing unit fabricated from modular, transportable components; replaces grid-powered instrumentation with a solar-powered programmable logic controller (PLC) driving low-power turbidity, pH and level sensors; replaces laboratory-cycle quality control with the field-deployable ML ensemble of Section 2.2, retrained on locally collected discharge and sediment data before operational use; and couples the resulting system to ENFEN/SENAMHI early-warning feeds so that binder dosing and mixing-unit deployment can be scheduled ahead of forecast El Niño-driven sediment surges.

2.5 Ethical statement and disclosure of language-model use

This manuscript is a literature-based engineering synthesis and design proposal; it does not involve human participants, animal subjects, identifiable personal data, or primary field sampling conducted by the author, and therefore formal research-ethics-committee approval is not applicable. All water-quality figures cited from the Rimac and Ichu basins are secondary data taken from the published, openly accessible sources listed in the References. In accordance with editorial policy on the use of large language models, an LLM was used exclusively for language editing, formatting and reference verification; the engineering framework, formula selection, comparative-matrix design and interpretation were conceived and carried out by the author, who takes full responsibility for the content.

3. Results and Discussion

Because this article synthesizes rather than generates primary experimental data, the following results are documented values and procedures drawn from the cited, DOI-verified sources, organized into a comparative matrix (Table 1) that juxtaposes Asian (predominantly Chinese) documented practice against the proposed Peru-adapted configuration across the four pillars of the framework. No statistical inference is claimed beyond what is reported in the original sources; the matrix is offered as a synthesis tool to support the engineering framework proposed in Section 2, and any figures should be read as literature-documented benchmarks rather than as results of new experiments performed for this article.

3.1 Comparative matrix of documented Asian practice and proposed Peru adaptation

Table 1

Comparative matrix of documented Asian (predominantly Chinese) practice versus the proposed low-cost adaptation for Andean rivers and lagoons of Peru, organized by the four pillars of the Sky–Land–Water–AI framework, compiled from the cited DOI-verified sources.

Pillar	Documented Asian practice	Proposed Peru adaptation	Key source(s)
Low-emission binders & micro-mechanisms	GGBS/fly-ash/carbide-slag composite binders partially replace OPC in centralized batching plants; humus amendment reduces exchangeable heavy-metal fraction in river sediment (Shanghai).	Modular, transportable mixing unit dosing the same composite binders in small batches at the descolmatation site; humus/organic amendment where locally available.	Wang et al. 2018; Gao et al. 2023
Machine-learning trend forecasting	Multi-model ensembles (RF, GBM, XGBoost, deep learning) trained on laboratory UCS/leachability datasets to forecast strength development and reduce testing burden.	Same ensemble architecture retrained on locally collected Peruvian discharge, binder-dosage and sediment data before field use; deployed on a low-power edge device.	Abdullah et al. 2024; Zhang et al. 2026; Luo et al. 2025
Sky–Land–Water–AI monitoring	Space–air–ground integrated remote-sensing network (satellite + drone + ground hyperspectral stations) for suspended-sediment monitoring, grid-powered, continuous laboratory support.	Solar-powered PLC with low-power turbidity/pH/level sensors and periodic drone survey; satellite tasking used opportunistically; coupled to ENFEN/SENAMHI early warning.	Hou et al. 2024; Chen et al. 2023
Co-solidification of multiple contaminants	Combined solidification/stabilization plus chemical oxidation to immobilize heavy metals and organic pollutants within the same treatment train; documented for co-contaminated Chinese soils.	Same combined-treatment logic applied to Rimac/Ichu-type sediment where mining-derived heavy metals and organic pollution co-occur, dosed via the mobile mixing unit.	Ma et al. 2018; Minga et al. 2023; Zárate-Cáceres et al. 2026

3.2 Framework architecture

Table 1 shows that composite low-emission binders (GGBS, fly ash, carbide slag) consistently reduce carbon footprint and alkalinity relative to pure-OPC stabilization while preserving or improving contaminant immobilization (Wang et al. 2018; Gao et al. 2023), and that multi-model ML ensembles are the documented approach of choice for forecasting UCS and leachability trends in stabilized soils and sediments across the cited studies (Abdullah et al. 2024; Zhang et al. 2026; Luo et al. 2025). These documented patterns motivate the coupled architecture in Figure 1, in which Sky–Land–Water sensing layers feed a common ML ensemble that forecasts strength, leachability and turbidity trends and, in turn, drives a low-emission-binder dosing controller — rather than treating monitoring, forecasting and binder dosing as independent design problems.

3.3 Constructive adaptation for Peru under El Niño 2026

The Rimac and Ichu basin data in Table 1 indicate that Peruvian field conditions combine legacy mining-related heavy-metal loads with organic pollution and oxygen depletion (Minga et al. 2023; Zárate-Cáceres et al. 2026), a co-contamination pattern consistent with the combined solidification/chemical-oxidation approach documented for Chinese soils (Ma et al. 2018) and with the humus-amended cement stabilization documented for heavy-metal-contaminated river sediment in Shanghai (Gao et al. 2023). As of mid-2026, ENFEN and the World Meteorological Organization have identified a high probability of an El Niño event through the remainder of the year, with Peruvian authorities prioritizing the cleaning and descolmatation of rivers, quebradas and drainage systems as a preventive measure; this reinforces the case for a transportable, solar-powered, ML-forecast-driven configuration of the kind illustrated in Figure 2, which can be deployed ahead of forecast sediment surges rather than only in reactive post-event cleanup.

3.4 Limitations

This article does not report new laboratory or field measurements; all binder-performance, ML-forecasting and monitoring figures discussed in Section 3 originate from the cited sources and were obtained under conditions (sediment matrices, contaminant mixtures, instrumentation, basin hydrology, grid access) that differ from those of Peruvian Andean systems. The ML ensemble described in Section 2.2 has been validated for UCS and leachability prediction in the source studies, but not yet retrained or field-validated on Peruvian discharge and sediment data. Direct comparability between documented Asian full-scale performance and its expected performance on Andean, multi-pollutant, high-altitude, El Niño-affected systems should therefore be treated as a working hypothesis rather than an established result. Pilot-scale field validation in a Peruvian basin, with locally collected influent characterization, binder-dosing trials and sediment gauging, is identified as the necessary next step before full-scale deployment.

4. Conclusions

This Method Article compiled documented, DOI-verified evidence on low-emission composite binders, multi-model machine-learning forecasting of stabilized-sediment strength and leachability, Sky–Land–Water–AI monitoring architectures, and multi-contaminant co-solidification practice, and used it to construct an integrated engineering framework formalized through an exponential strength–binder-ratio law, a solid–liquid partition/immobilization coefficient for co-contaminants, a weighted multi-model ML ensemble equation, and a carbon-footprint reduction metric. The evidence compiled indicates that composite binders such as GGBS, fly ash and carbide slag can reduce the carbon footprint of sediment stabilization relative to pure OPC while maintaining contaminant immobilization, that multi-model ML ensembles improve strength- and leachability-trend forecasting over single-model baselines, and that Peruvian basins such as the Rimac and Ichu already exhibit heavy-metal pollution indices above critical

contamination thresholds. Building on this evidence, and in light of the high-probability El Niño event identified by ENFEN for 2026, constructive procedures documented for Asian full-scale deployments were translated into a proposed low-cost, solar-powered, modular configuration adapted to the topography and resource constraints of Andean rivers and lagoons. The framework is a design-and-synthesis proposal; its central limitation is the absence of primary experimental validation on Peruvian systems, which is proposed as the immediate follow-up study.

Declarations

Ethics approval and consent to participate: Not applicable. This is a literature-based engineering synthesis; no human participants, animal subjects or primary field/laboratory data collection were involved.

Consent for publication: Not applicable.

Funding: The author declares that no external funding was received for this work.

Competing interests: The author declares no competing interests.

Author contributions: P.R.P.G. is the sole author and is responsible for conceptualization, methodology, formal analysis, writing, and figure preparation.

Data availability: All data generated or analysed during this study are included in this published article.

References

1. Abdullah GMS, Ahmad M, Babur M, Badshah MU, Al-Mansob RA, Gamil Y, Fawad M. Boosting-based ensemble machine learning models for predicting unconfined compressive strength of geopolymer stabilized clayey soil. Sci Rep. 2024;14:2323. https://doi.org/10.1038/s41598-024-52825-7.
2. Chen S-L, Chou H-S, Huang C-H, Chen C-Y, Li L-Y, Huang C-H, Chen Y-Y, Tang J-H, Chang W-H, Huang J-S. An intelligent water monitoring IoT system for ecological environment and smart cities. Sensors. 2023;23(20):8540. https://doi.org/10.3390/s23208540.
3. Gao H, Tao H, Yang Y, Che Q, Tang Q, Gu Y. Effect of humus on the solidification and stabilization of heavy metal contaminated river sediment. Int J Environ Res Public Health. 2023;20(6):4882. https://doi.org/10.3390/ijerph20064882.
4. Hou Y, Ma Y, Hou Z, Arif M, Li J, Ming X, Liu X, Xing Q. Space–ground remote sensor network for monitoring suspended sediments in the Yellow River basin. Sensors. 2024;24(21):6888. https://doi.org/10.3390/s24216888.
5. Luo Z, Xue X, Xiong C, et al. Data-driven prediction of unconfined compressive strength in stabilized soils using machine learning. Discover Appl Sci. 2025;7:1122. https://doi.org/10.1007/s42452-025-07766-9.

6. Ma Y, Liu Z, Xu Y, Zhou S, Wu Y, Wang J, Huang Z, Shi Y. Remediating potentially toxic metal and organic co-contamination of soil by combining in situ solidification/stabilization and chemical oxidation: efficacy, mechanism, and evaluation. Int J Environ Res Public Health. 2018;15(11):2595. https://doi.org/10.3390/ijerph15112595.
7. Minga JC, Elorza FJ, Rodriguez R, Iglesias A, Esenarro D. Assessment of water resources pollution associated with mining activities in the Parac subbasin of the Rimac River. Water. 2023;15(5):965. https://doi.org/10.3390/w15050965.
8. Wang L, Yu KQ, Li J-S, Tsang DCW, Poon CS, Yoo J-C, Baek K, Ding S, Hou D, Dai J-G. Low-carbon and low-alkalinity stabilization/solidification of high-Pb contaminated soil. Chem Eng J. 2018;351:418–27. https://doi.org/10.1016/j.cej.2018.06.118.
9. Yang J, Sun F, Su H, Tao Y, Chang H. Multiple risk assessment of heavy metals in surface water and sediment in Taihu Lake, China. Int J Environ Res Public Health. 2022;19(20):13120. https://doi.org/10.3390/ijerph192013120.
10. Zárate-Cáceres CR, Iparraguirre-Meza M, Pérez-Venegas CJ, Picoy-Gonzales JA, Ordoñez-Ccora G, Lacho-Gutiérrez P, Riveros-Laurente KY, Díaz-Aranda DL, Gutiérrez-Iparraguirre GG, Huarcaya-Taype R et al. (2026). Integrated water quality assessment and health risk analysis of heavy metal and microbial contamination in the Ichu River, Peru. F1000Research. https://doi.org/10.12688/f1000research.162022.4
11. Zhang J, Hu G, Zhang J, Wu J. Prediction of the unconfined compressive strength of one-part geopolymer-stabilized soil under acidic erosion: comparison of multiple machine learning models. Materials. 2026;19(1):209. https://doi.org/10.3390/ma19010209.

Figures

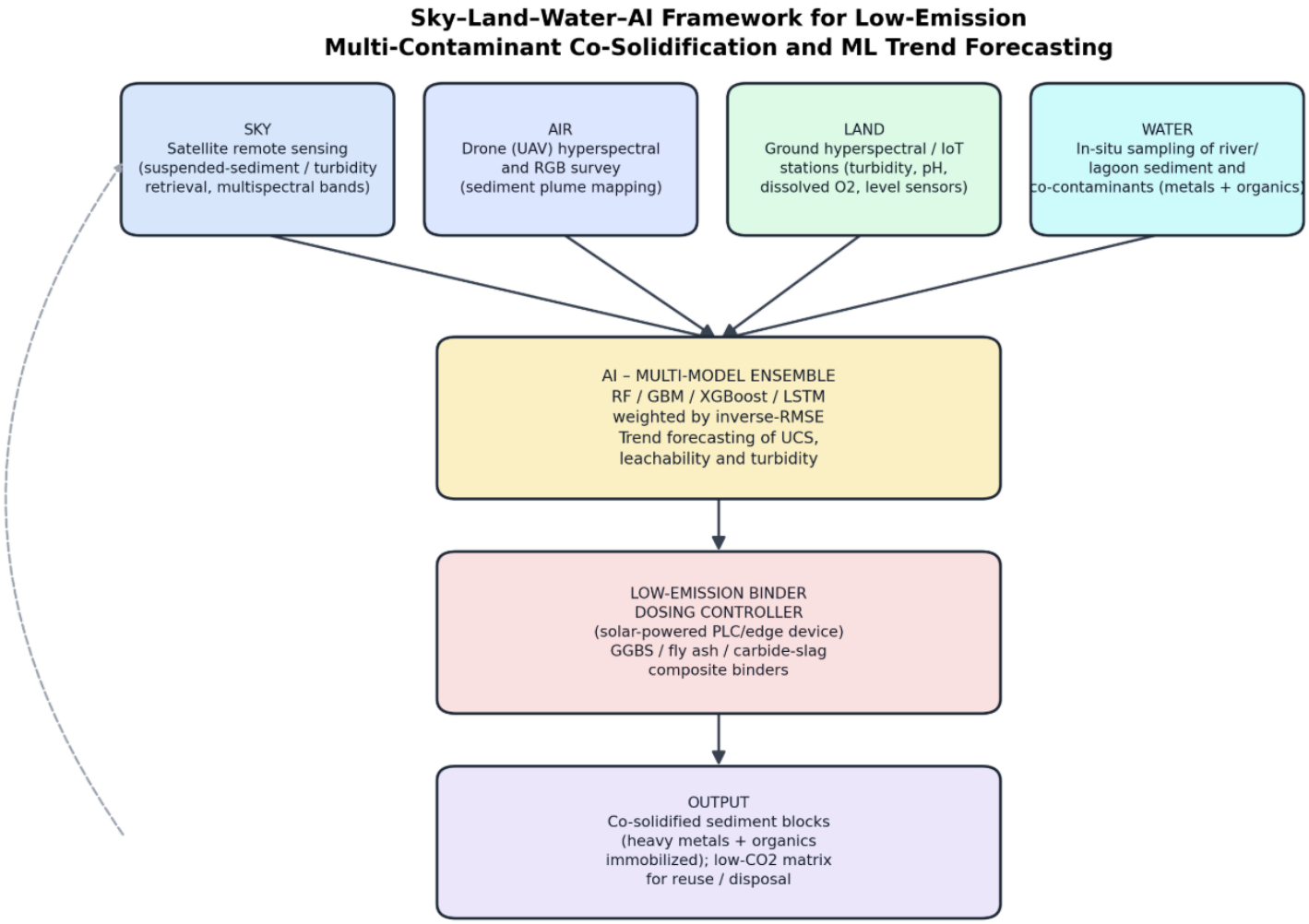


Figure 1. Sky–Land–Water–AI monitoring-to-solidification architecture (schematic, design-synthesis proposal).
Figure authored by Paul Ricardo Prudencio Gálvez. All rights reserved.

Figure 1

See image above for figure legend.

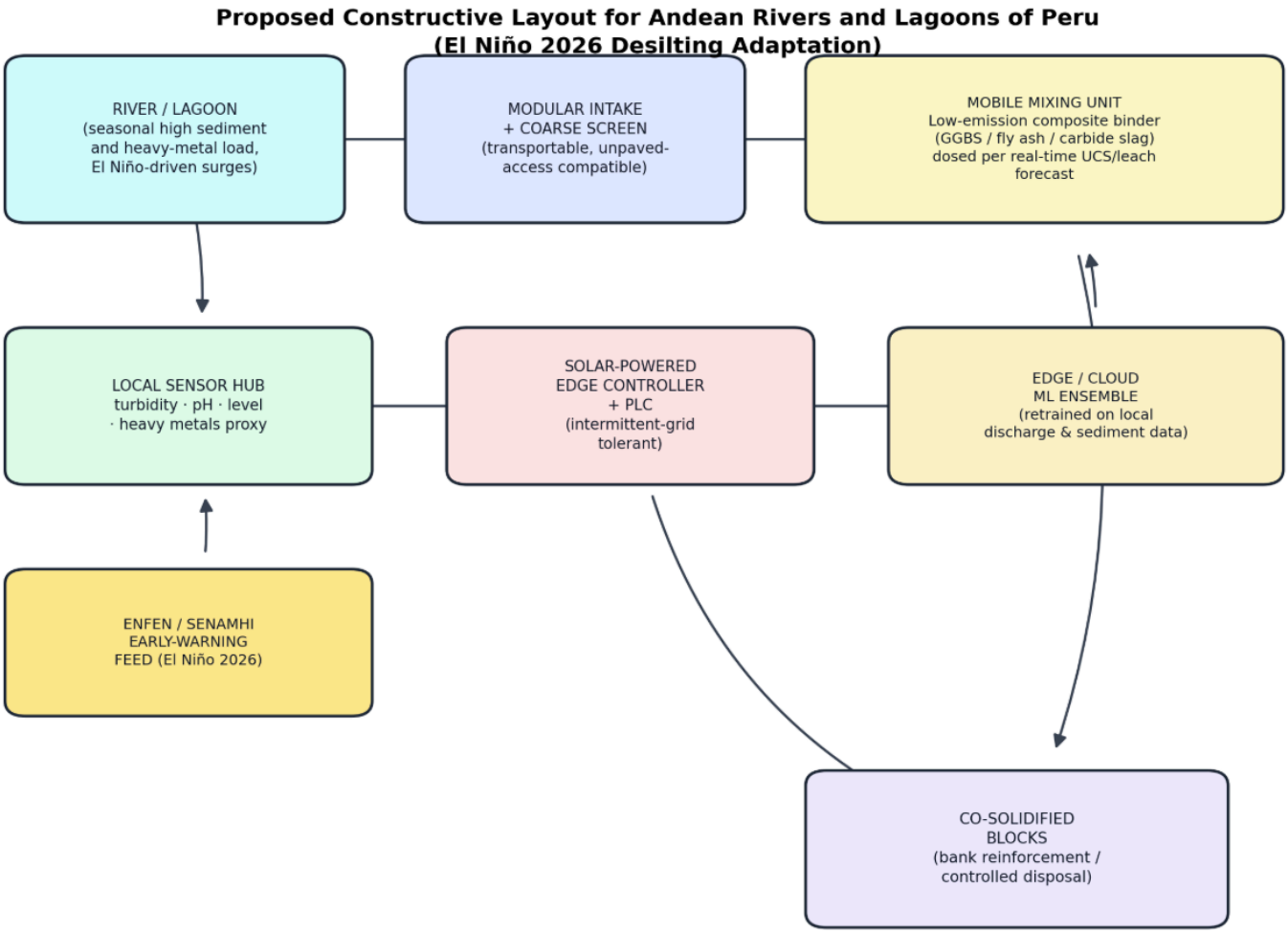


Figure 2. Constructive layout, tools and material sequence proposed for deployment of the modular co-solidification unit in Andean rivers and lagoons of Peru under El Niño 2026 desilting demand.
Figure authored by Paul Ricardo Prudencio Gálvez. All rights reserved.

Figure 2

See image above for figure legend.